Spectrochimica Acta Part B 116 (2016) 8–15

Contents lists available at ScienceDirect

Spectrochimica Acta Part B

journal homepage: www.elsevier.com/locate/sab

Wavelength dependency and threshold measurements for nanoparticle-enhanced laser-induced breakdown spectroscopy

Ashraf M. EL Sherbini [a], Christian G. Parigger [b,*]

[a] Laboratory of Laser and New Materials, Faculty of Science, Cairo University, Giza, Egypt
[b] The University of Tennessee/University of Tennessee Space Institute, Center for Laser Applications, 411 B.H. Goethert Parkway, Tullahoma, TN 37388-9700, USA

ARTICLE INFO

Article history:
Received 13 September 2015
Accepted 17 November 2015
Available online 2 December 2015

Keywords:
Nanoparticles
Laser ablation
Atomic spectroscopy
Zinc monoxide
Laser-induced breakdown spectroscopy

ABSTRACT

Nanoparticles of zinc monoxide are selected for laser-induced breakdown spectroscopy with 5 ns pulsed 1064 nm, 532 nm, and 355 nm radiation from a Nd:YAG laser device. Fluences of 2 to 20 J/cm^2 are used, and plasma conditions are determined by recording emission spectra in the temporal window of 1 to 2 μs after optical breakdown initiation. The bulk- *versus* nano-particle plasmas in laboratory air show that the averaged electron density and temperature values are practically identical. Enhanced signals are recorded for nanoparticles in the amount of ×10 to ×120 for 355 nm radiation. The nanoparticles cause lower optical breakdown thresholds and show signal enhancements as evidenced from the analysis of the Zn I line at 481.0 nm. The measured H_α line at 656.3 nm usually occurs in laser-induced plasma experiments in standard ambient temperature and pressure laboratory air, and it is used in the interpretation of the bulk- and nanomaterial results. The theoretical model largely predicts and confirms the excitation wavelength-dependent experimental results.

1. Introduction

The generation of laser-induced plasma [1–3] requires above-threshold peak irradiance of the order of 100 GW/cm^2 for standard ambient temperature and pressure (SATP) air. The thresholds are lower by several orders of magnitude for aerosol- and/or nanoparticle-laden laboratory air [4], moreover, can be further reduced for solid materials. The laser-induced plasma at or near the surface emits radiation. In plasma spectroscopy, electron density and temperature are usually determined to describe the plasma conditions [5]. The analysis of the emitted plasma radiation is generally called optical emission spectroscopy (OES), or specifically, laser-induced breakdown spectroscopy (LIBS) [2]. Desired outcomes of LIBS include elemental identification, composition and concentration of the investigated sample [1–3]. For the application of LIBS as an analytical technique, it continues to be desirable to increase the sensitivity to allow one to investigate significantly diluted concentrations with a limit of detection (LOD) of the order of a few parts-per-million [1,6]. In order to improve the LOD one can engage in efforts that decrease the background contributions originating from continuum radiation or from random instrumental noise, or alternatively, one can design methods that increase the signal intensity. A variety of approaches were studied with the objective to enhance the value of LIBS in analytical chemistry including the use of double pulse techniques in collinear and orthogonal arrangements [7,8], and use of ultra-short laser pulses [9] with considerable LOD improvements [6].

The addition of a thin layer of nanomaterial composed of noble elements to a solid material surface can be favorable for measurement of increased signals, as previously recognized [10]. The enhanced emission has been explained qualitatively in terms of the action of the localized surface plasmon resonance (LSPR) [10]. However, the interaction of laser radiation with nanomaterials and corresponding bulkmaterials has been investigated recently. Under otherwise the same experimental arrangements and conditions, extensive systematic experimental works employed OES for different laser parameters and time delays [11–14]. Several conclusions were communicated, including: (1) the enhanced emission from the nanomaterials increases linearly with time delays when compared with bulkmaterial; (2) the enhanced emission increases with decreasing laser fluence; (3) there are no apparent changes of the plasma electron density and temperature; and (4) the enhancement factors that may vary for different experimental conditions can be associated with the relative masses ejected from both targets. Detailed experimental studies by De Giacomo *et al.* [13,14] indicate that the addition of thin layer of nanomaterial composed of noble elements on a metallic target surface reduces the threshold for plasma generation [3,15].

Previous communications elaborate that the enhanced emission can be attributed to the physical properties offered by the new nanomaterials when irradiated at peak power levels capable of generating optical breakdown [12]. The possibility of more efficient transfer of radiation to the target has been recognized including the application of lower laser fluence for nanomaterial than required for bulkmaterial that is analyzed with LIBS.

In this article, new results of the enhanced emission characteristics are presented. Nanomaterial enhanced LIBS (NELIBS) is explored in

* Corresponding author.
E-mail address: cparigge@tennessee.edu (C.G. Parigger).

http://dx.doi.org/10.1016/j.sab.2015.11.006
0584-8547/

terms of dependency on the laser wavelengths of 1064 nm, 532 nm, and 355 nm and in terms of the required threshold laser fluence. The experimental work is conducted for the fixed time delay of 1 μs from optical breakdown and for a gate width of 1 μs. In the analysis, a refined threshold equation is introduced to predict the plasma thresholds as function of the excitation wavelength and the nanomaterial particle diameter.

2. Experimental details

The experimental setup is similar to the one described in Refs. [11, 12]. Fig. 1 illustrates the arrangement. It is comprised of a Nd:YAG laser device that delivers a maximum energy of 680 mJ within a 5 ns pulse duration at the fundamental wavelength of 1064 nm.

The pulse energy was attenuated with a set of absorbing sheets that are introduced near the focusing lens. A laser beam spotsize of radius 1 ± 0.1 mm was used for 1064 nm. The other two harmonics at the wavelengths of 532 nm and 355 nm were operated at the maximum output energies of 180 and 95 mJ per 5 ns pulse and were focused to spot sizes of equal radii of 0.55 ± 0.07 mm in order to obtain the same range for the laser fluences.

In the experiment, the laser spot sizes for the three laser wavelengths are measured using thermal paper supplied by Quantel *R* for the different harmonics. In order to reach constant fluence conditions, the laser focusing lens position was carefully adjusted. A quartz beam splitter was utilized to monitor the incident laser peak irradiance. The beam splitter reflects 4% and absorbs 4% of radiation as recorded with the use of an absolutely calibrated power-meter (Ophier model 1z02165). The emitted radiation from the nano- and bulkmaterials was collected with an optical fiber of inner diameter of 25 μm that was placed at a distance of 15 mm from the plasma expansion axis. Spectra were recorded with an Echelle type spectrograph (SE200 from Catalina) in conjunction with a time-gated ICCD camera (Andor- iStar- model DH734-18F). The gate-open time and the time delay from the laser-induced plasma were adjusted to 1 μs using the control software KestrelSpec 3.9.

The absolute sensitivity calibration of the spectrograph-camera system in the wavelength range from 300 to 900 nm was accomplished with a standard Deuterium-Halogen lamp (Ocean optics *R*-DH2000-CAL). The wavelength calibration and spectrograph bandwidth in the amount of 0.12 nm were measured using a low pressure Hg lamp (Ocean optics model HG1). The nano- and bulk-ZnO target materials were pressed into shapes of tablets. The supplied bulktarget consisted of irregularly shaped crystals with sizes of the order of a few mm. The crystals were put into a mold and compressed into cylindrical shape of the same thickness as the compressed nano targets. A primarily solid structure resulted for the compressed crystals, referred to as "bulk" material, and a relatively dense but loosely-packed structure was achieved for the nanoparticles, referred to as "nano" material. The targets were prepared in standard ambient temperature and pressure laboratory air, thereby possibly trapping air moisture as well. While hydrogen lines are typically observed in micro-plasma generated with naonosecond laser radiation in air, trapped moisture could contribute to the observed hydrogen alpha line over and above the contributions from the air. Careful future investigations are expected to address this extra source for the appearance of the hydrogen alpha line. A so-called xy ϕ-holder was used to mount and move the targets and to ensure a fresh target area for each laser shot. The strongest neutral Zn I line at the wavelength of 481.01 nm was selected to monitor the plasma emissions for the different wavelengths and especially for lower fluences of the order of a few J/cm^2. Typically, the ZnO (MKNANO-ZnO-030) materials of almost spherically shaped powder samples of diameter $D \simeq$ 30 nm were purchased from "MK$_{NANO}$®", and were used in the studies without further purification or applying heat treatments.

3. Results and discussion

The analyses of the recorded data from nano- and bulkmaterials are geared towards evaluation of the temperature, electron density and ground state population ratios from the recorded spectra. Results for the threshold values are presented after the basic elements for the modeling are introduced.

3.1. Relative plasma parameters

In order to determine which one or possibly more of the plasma parameters are likely causing enhanced emission signals, electron density, n_e, and temperature, T_e, as well as particle density, N_0, are measured. More specifically, direct measurements were performed of the relative plasma parameters T_e^N/T_e^B, n_e^N/n_e^B and N_0^N/N_0^B, where the superscripts *N* and *B* denote nano- and bulkmaterial, respectively.

Fig. 2 illustrates an overview of typical results that were recorded for various experimental conditions. The plasma emission was monitored using the Zn I line at 481 nm. Enhanced emissions occur for shorter laser wavelengths and show an up to $\times 120$ increase at a laser fluence of 2 J/cm^2, and larger enhancements occur for the smaller plasma initiation wavelengths.

Relative electron temperature

Measurement of the electron temperatures and hence the ratio T_e^N/T_e^B can be accomplished by constructing a multi-element Boltzmann plot. Spectral intensities of the observed Zn I lines from both nano- and

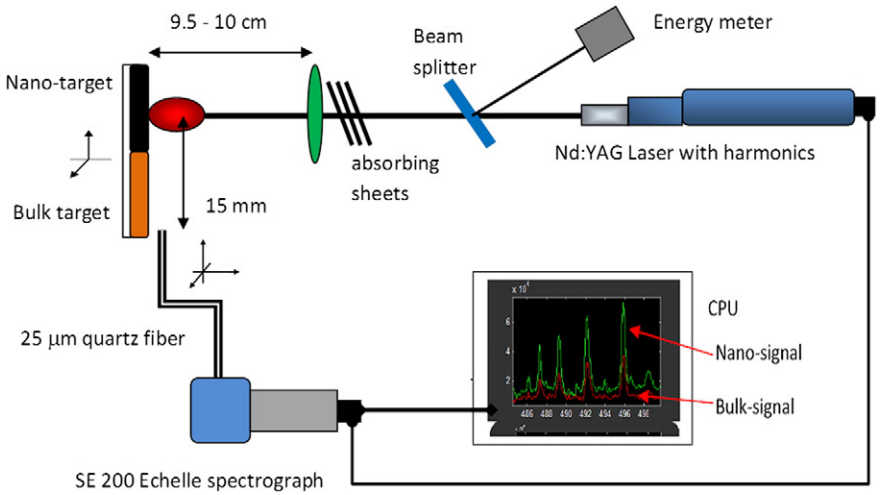

Fig. 1. Experimental arrangement.